



Cortical layer-dependent dynamic blood oxygenation, cerebral blood flow and cerebral blood volume responses during visual stimulation

Tao Jin ^{a,*}, Seong-Gi Kim ^{a,b}

^a Department of Radiology, 3025 East Carson Street, University of Pittsburgh, Pittsburgh, PA 15203, USA

^b Department of Neurobiology, University of Pittsburgh, Pittsburgh, PA 15203, USA

ARTICLE INFO

Article history:

Received 16 January 2008

Revised 17 June 2008

Accepted 24 June 2008

Available online 4 July 2008

Keywords:

fMRI

BOLD

CBV

CBF

Cortical lamina

Visual stimulation

MION

Post-stimulus undershoot

ABSTRACT

The spatiotemporal characteristics of cerebral blood volume (CBV) and flow (CBF) responses are important for understanding neurovascular coupling mechanisms and blood oxygenation level-dependent (BOLD) signals. For this, cortical layer-dependent BOLD, CBV and CBF responses were measured at the cat visual cortex using fMRI. Major findings are: (i) the time-dependent fMRI cortical profile is dependent on imaging modality. Overall, the peak across the cortex occurs at the cortical surface for BOLD, but at the middle cortical layer for CBV and CBF. Compared to an initial stimulation period (4–10 s), the spatial specificity of CBV to the middle cortical layer increases significantly at a later time, while the specificity of BOLD and CBF slightly changes. (ii) The CBV response at the upper cortical area containing large pial vessels has a faster onset time and time to peak than the BOLD response at the same area, and a faster time to peak than CBV at the middle cortical area with microvessels. This suggests that the dilation of microvessels at the middle cortical area follows arterial volume increase at the surface of the cortex. (iii) For all three modalities, the post-stimulus undershoot was observed with the 60-s stimulation paradigm, indicating that the post-stimulus BOLD undershoot cannot be explained by the delayed venous CBV recovery theory under our experimental conditions. (iv) The relationship between CBV and CBF responses is both spatially and temporally dependent. Thus, a single power-law scaling constant (gamma value) may not be applicable for high-resolution study.

© 2008 Elsevier Inc. All rights reserved.

Introduction

The blood oxygenation level-dependent (BOLD) functional magnetic resonance imaging (fMRI) contrast (Ogawa et al., 1990) arises from a combination of neural activation-induced changes in oxygen metabolism and hemodynamic responses, such as cerebral blood flow (CBF) and volume (CBV). Because temporal and spatial characterization of hemodynamic changes is essential for understanding BOLD signals and can provide insights into neurovascular controlling mechanisms, extensive research has been carried out; however, on several issues conclusive understanding is still lacking.

Spatial specificity of fMRI signals is dependent on the source of imaging signals. Since the BOLD signal is sensitive to large draining veins, improved specificity to the parenchyma may be achieved by using only the early response before stimulation-induced deoxyhemoglobin changes reach large draining veins (Goodyear and Menon, 2001). Based on time-dependent intrinsic optical imaging studies in rat somatosensory cortex, Sheth et al. suggested that spatial specificity of BOLD and CBV signals is optimal within the first 2 to 3-s window following stimulation (Sheth et al., 2004). In fMRI, in contrast, CBV response at steady state has been found to be fairly specific to the

parenchyma for long stimulation (>10 s), and is relatively localized to the middle cortical layer where the microvessel density is the highest (Harel et al., 2006; Lu et al., 2004b; Zhao et al., 2006). Therefore, it is important to examine the time-dependent spatial specificity of fMRI signals.

Dynamic properties of fMRI signals may provide information about the source of responding vasculature. Currently, comparison between BOLD and CBV dynamics in animals is inconclusive: slower CBV response during stimulation compared to BOLD (Leite et al., 2002; Mandeville et al., 1998) vs. faster CBV response (Harel et al., 2002; Silva et al., 2007). A post-stimulus signal undershoot is often observed in the BOLD response, but the post-stimulus response of CBV is controversial. Mandeville et al. reported that the post-stimulus return of CBV response to baseline is much slower than the BOLD response (Leite et al., 2002; Mandeville et al., 1998), while a relatively fast return of CBV was reported in a very recent measurement (Frahm et al., 2008). The above-mentioned discrepancies of relationships between BOLD and CBV may partly be due to the differences in spatial localization (Yacoub et al., 2006). Thus, it will be necessary to acquire BOLD and CBV responses using MRI with high spatial resolution to shed light on these controversies.

The relationship between CBV and CBF responses during brain activation is important for understanding neurovascular coupling, and is often used for calculation of the oxygen metabolism change

* Corresponding author. Fax: +1 412 383 6799.

E-mail address: taj6@pitt.edu (T. Jin).

(Kim and Ugurbil, 1997). Due to the difficulty in measuring both CBV and CBF on the same subjects, the relative changes in CBV and CBF were assumed to be tightly coupled in many studies (Davis et al., 1998; Hoge et al., 1999a; Kim et al., 1999). The quantitative relationship between relative CBV ($rCBV$) and relative CBF values ($rCBF$) at a steady state condition was described as: $rCBV = rCBF^\gamma$, where γ is often assumed to be a fixed value of 0.38 from the hypercapnic results in anesthetized monkeys (Grubb et al., 1974). Recently, γ was found to be dynamically changed during the forepaw stimulation period in the rat somatosensory cortex (Kida et al., 2007), and to be region-specific under hypercapnia in the rat brain (Wu et al., 2002). Thus, for dynamic high-resolution oxygen metabolism measurements, it is necessary to study the spatiotemporal characteristics of the $rCBV$ and $rCBF$ relationship.

In this study, a well-established cat visual stimulation model was used to investigate the spatiotemporal characteristics of BOLD, CBV, and CBF responses. Although fMRI does not offer the spatial resolution of different vascular compartments, the signals can be analyzed by different cortical layers of the cat visual cortex: the middle cortical layer contains mostly microvessels, such as small arterioles, capillaries, and small venules; while the upper cortical layer contains more large vessels such as arteries and veins. The cortical layer dependence of BOLD, CBV and CBF responses was investigated as a function of time, and the spatial specificity of functional maps at different time periods during stimulation was also analyzed. Commonly observed post-stimulus BOLD undershoot was compared with post-stimulus responses of CBV and CBF in order to determine whether venous volume contribution is the major source for the BOLD undershoot. Additionally, the relationship between CBV and CBF responses was investigated as a function of cortical depth and time.

Materials and methods

General preparation

Nine female adolescent cats weighing 0.75–2.4 kg were used in a total of sixteen imaging sessions with the approval of the Institutional Animal Care and Use Committee at the University of Pittsburgh; three animals were used for more than one session. Animals were anesthetized under 0.8–1.3% isoflurane and artificially respired in a 7:3 medical air/O₂ mixture. The end-tidal CO₂ level was kept within 3.5±0.5%, and the rectal temperature was controlled at 38.5±0.5 °C using a water-circulating pad. The femoral or cephalic vein was cannulated to deliver fluid with pancuronium bromide (~0.2 mg/kg/h). The animal's head was fixed with a homemade head frame with bite and ear bars. For fMRI study, the visual stimulus was high contrast black and white square-wave gratings (spatial frequency of 0.15 cycle/degree) drifting with a temporal frequency of 2 cycles/s. Stationary gratings of the same spatial frequency were presented for the control.

MR data acquisition

All MRI experiments were performed on a 9.4 T/31 cm horizontal magnet (Magnex, UK) interfaced to a Unity INOVA console (Varian, Palo Alto, CA). Fast low-angle shot (FLASH) images were used to place the region of interest (ROI) close to the isocenter of the magnetic field. Magnetic field homogeneity was optimized by localized shimming (~10×5×5 mm³ in volume) over the visual cortex to yield a narrow water spectral linewidth (<25 Hz). From multi-slice "scout" gradient-echo (GE) BOLD fMRI studies, a single 2-mm coronal plane nearly perpendicular to the surface of the cortex, which gave a high quality echo planar image as well as robust BOLD contrast, was chosen. All subsequent experiments were conducted on that slice with a 2×2 cm² field of view and a 2 mm thickness. For anatomical reference, a T₁-weighted image was acquired by a 4-segmented inversion recovery

spin-echo, echo planar imaging (EPI) technique with a 128×128 matrix.

BOLD, CBV-weighted and CBF fMRI experiments were performed with 20-s and 60-s block-design stimulation paradigms. The 20-s stimulation paradigm consisted of 20 s control, 20 s stimulation, and 50 s control, while the 60-s stimulation paradigm consisted of 60 s control, 60 s stimulation, and 160–162 s control. 20-s and 60-s stimulus BOLD and CBV-weighted fMRI data ($n=6$ sessions from 4 animals) were obtained at the same imaging session, while 20-s CBF ($n=5$ sessions from 4 animals) and 60-s CBF studies ($n=5$ sessions from 4 animals) were separately performed due to the need of sufficient signal averaging within a limited experimental time.

BOLD and CBV-weighted fMRI studies

BOLD and CBV-weighted images were obtained using a 1.6-cm diameter surface coil before and after the injection of 10 mg/kg monocrystalline iron oxide nanoparticles (MION), respectively. A two-segmented GE EPI sequence was used with repetition time (TR)=0.5 s/segment and a 96×96 matrix size. Runs with 20-s and 60-s stimulations were interleaved. For 20-s stimulation studies with a temporal resolution of 1 s, BOLD and CBV-weighted fMRI were acquired with echo times (TE) of 20 ms and 10 ms, respectively. For 60-s stimulation studies, two TEs of 10 ms and 20 ms were arrayed for BOLD, and two TEs of 6 ms and 10 ms for the CBV-weighted fMRI studies; thus, the effective temporal resolution was 2 s. About 20 runs were averaged for each stimulation condition.

CBF fMRI studies

Functional CBF responses were measured with the Flow-sensitive Alternating Inversion Recovery (FAIR) technique (Kim, 1995). FAIR images were obtained by alternatively acquiring slice-selective and non-slice-selective inversion recovery (IR) images using an actively detunable two-coil system, where a Helmholtz head coil was used for inversion and a 1.6 cm surface coil for excitation and reception. The order of slice-selective and non-slice-selective inversion was reversed after each run. A Gaussian-shaped adiabatic pulse with an R -value of 100 was used to obtain a sharp profile of the 6 mm thick inversion slab (Garwood and Delabarre, 2001). Single-shot GE EPI was used with matrix size=64×64, TE=19 ms, TR/TI=2.5 s/1.25 s for 20-s stimulation studies, and TR/TI=3.0 s/1.5 s for 60-s stimulation studies. About 50 runs were averaged for each study.

Data analysis

Data were first zero-filled to a 128×128 matrix and Fourier-transformed, then all functional runs under the same experimental conditions were averaged. From FAIR measurements, CBF-weighted images were obtained by subtracting non-slice-selective IR images from neighboring slice-selective IR images and averaging two runs with a reversed order of non-slice-selective and slice-selective inversion, resulting in a nominal temporal resolution of 2.5 and 3.0 s for 20-s and 60-s stimulation studies, respectively. Except for the CBF data that are insensitive to baseline signal drift (Kim, 1995), linear detrending was performed using the pre-stimulation data from a ROI covering most gray matter areas in the imaging slice (e.g., the green contours in Fig. 1). All data are reported as mean±standard deviation (SD), unless otherwise noted.

Student's t -test was performed using STIMULATE software (Strupp, 1996) on a pixel-by-pixel basis to detect activation, where pre-stimulus data were considered as control state, and data ≥3 s after the stimulus onset as activated state. A P -value threshold of 0.05 (uncorrected for multiple comparisons) was adopted, and a minimal cluster size of three pixels was applied. Percentage signal changes were then calculated for the statistically active pixels.

In the CBV-weighted data, the contribution from the change of deoxyhemoglobin content (Kennan et al., 1998) can be significant at

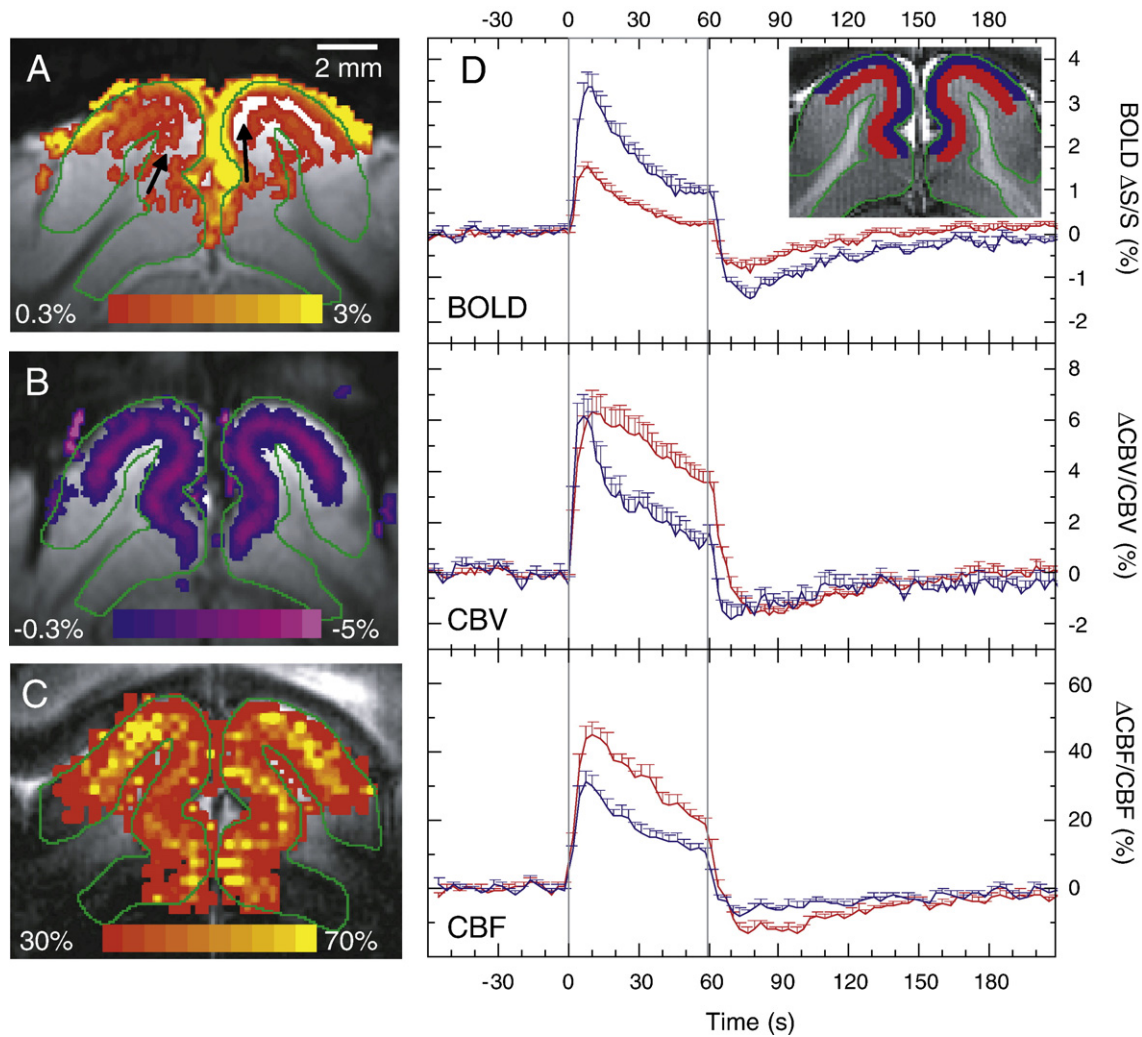


Fig. 1. Percentage change maps of BOLD (A), CBV-weighted (B), and CBF (C) responses for 60-s stimulation. (A and B) were obtained from one representative animal, and (C) was from another animal. During visual stimulation, BOLD and CBF signals increased mostly within the gray matter of primary visual cortex (outlined by green contours), while CBV-weighted signal decreased due to increasing amount of iron oxide particles within an imaging voxel. Highest BOLD change was located at the surface of the cortex. The BOLD signal was hardly detectable at the middle cortical area (arrows). (D) Averaged time courses of BOLD, CBV, and CBF percentage changes. The red and blue time courses were obtained from the middle and upper cortical ROI as indicated in the T_1 -weighted inset image, respectively. Time between two gray lines is the stimulation period. The middle cortical area had higher CBF and smaller BOLD responses compared to the upper cortical area. Error bar = standard error of the mean.

high magnetic fields, in particular at surface large vessel areas. Therefore, the correction of BOLD contribution was performed (Zhao et al., 2006). Initially, baseline relaxation rate change due to MION injections (without any stimulation) was calculated from the pre-stimulation data with two TE values before and after the MION injection, which was proportional to the baseline CBV value. Stimulation-induced relaxation rate changes (ΔR_2^*) of BOLD and CBV-weighted signals were calculated, and their difference was proportional to ΔCBV . For 60-s stimulation studies, ΔR_2^* was obtained from the difference between fractional signal changes of two TE data, divided by the difference between two echo times. For 20-s stimulation data, ΔR_2^* was calculated from fractional signal changes divided by TE, $-(\Delta S/S)/TE$. Since $\sim 30\%$ of GE BOLD fMRI signals with TE of 20 ms are likely due to the inflow effect and intravascular contributions based on previous multi-TE data obtained with similar imaging parameters (Jin et al., 2006), ΔR_2^* of extravascular BOLD signals was assumed to contribute to 2/3 of total BOLD signals. Then, CBV fractional changes were obtained by stimulation-induced ΔCBV divided by the baseline CBV (Zhao et al., 2006).

Quantitative analyses were performed on ROI using in-house Matlab® routines (Mathworks, Natick, MA). The same ROIs were

used for BOLD and CBV-weighted data, while separate ROIs were chosen for each CBF dataset. Signal changes were obtained from ROIs regardless of whether pixels passed the statistical threshold of activation. (i) To determine cortical-depth-dependent temporal responses, two ROIs were drawn from the anatomic image: the upper cortical area (UCA) and middle cortical area (MCA) ROIs were hand-traced, each with ~ 3 pixels thickness to encompass approximately the surface 1/3 and the middle 1/3 of gray matter, respectively. The MCA ROI contains mostly microvessels while the UCA ROI contains more large vessels and some partial volume of cerebrospinal fluid. Time courses obtained from both ROIs were compared. Peak intensity and time of post-stimulus undershoots were determined in addition to positive peak intensity. For the 60-s stimulation data, signal changes from 18 s to 60 s after the stimulus offset, normalized by the positive peak intensity, were averaged for each dataset. To examine time-dependent spatial specificity, the specificity index was calculated as a ratio between percentage signal changes of MCA and UCA for three different time periods: 4 to 10 s (TP1), 12 to 30 s (TP2), and 32 to 60 s (TP3). To determine onset time and time to peak (TTP), 20-s stimulation CBV and BOLD data were temporally interpolated to 200 ms resolution; then, times to 10% and

Table 1
Summary of BOLD, CBV and CBF peaks and post-stimulus undershoots^a

Modality	Region	Positive peak	Undershoot peak	TTU ^b	Undershoot/peak ^c
BOLD	UCA	3.5±0.7%	-1.5±0.4%	17.8±1.6 s	-0.23±0.09 (***)
	MCA	1.5±0.3%	-1.0±0.4%	16.0±4.0 s	-0.34±0.13 (**)
CBV	UCA	6.4±2.0%	-2.5±0.8%	13.3±4.8 s	-0.16±0.10 (*)
	MCA	6.5±2.0%	-1.9±0.5%	25.0±8.0 s	-0.20±0.05 (***)
CBF	UCA	32±7%	-9.6±3.5%	18.4±5.0 s	-0.17±0.06 (**)
	MCA	46±8%	-15±2.6%	23.6±5.5 s	-0.23±0.03 (***)

^a 60-s stimulation data were used to determine characteristics of post-stimulus undershoots in upper and middle cortical areas (UCA and MCA). All values were presented as mean±SD ($n=6$ for BOLD and CBV, and $n=5$ for CBF).

^b TTU: time to reach the undershoot peak after the stimulus offset.

^c The ratio of undershoot to peak was obtained from the average post-stimulus undershoot intensity over 18 to 60 s after stimulation offset, normalized by the positive peak intensity. Statistical significances are indicated as * ($P<0.05$), ** ($P<0.005$), and *** ($P<0.0005$).

90% of the peak were calculated for each individual dataset and considered as the onset time and TTP, respectively. (ii) For time-dependent cortical profile analysis, rectangular sections within area 18 of the visual cortex were first selected from the anatomical image (Bonhoeffer and Grinvald, 1993), then pixels were spatially interpolated along the direction normal to the cortical surface using the nearest-neighbor resampling method (Tsao, 2003). Cortical profiles were averaged for three time periods during 60-s stimulation. Finally the averaged signal profiles were plotted as a function of distance from the cortical surface. The normalized cortical profile was calculated by dividing the peak signal intensity of each data set. The cortical layer information was obtained from the relative distance from the cortical surface in area 18 (Payne and Peters, 2002).

To determine the spatiotemporal relationship between CBV and CBF, the power-law scaling constant γ was calculated by $\ln(rCBV)/\ln(rCBF)$, where time courses of relative CBV and CBF normalized by baseline values ($rCBV$ and $rCBF$, respectively) were temporally interpolated, taking into account their different temporal resolution. Note that $rCBV$ and $rCBF$ are equivalent to $(1+\Delta CBV/CBV)$ and $(1+\Delta CBF/CBF)$, respectively. Since the CBV and CBF data were obtained from different studies, standard error of the mean was calculated by propagation of CBV and CBF errors.

Statistical tests were performed to determine: (i) the temporally dependent spatial specificity index for BOLD, CBV, and CBF; (ii) the difference between the onset time and the TTP of each response at UCA and MCA; and (iii) the significance of the post-stimulus undershoots of the 60-s stimulation data. For the statistical test, a Student's t -test (paired or unpaired) or a Wilcoxon signed rank test was performed to evaluate the statistical significance, depending on whether the data were normally distributed. Bonferroni correction was applied for multiple comparisons.

Results

Spatiotemporal characteristics of BOLD, CBV and CBF responses

To compare functional maps of BOLD, CBV and CBF, 60-s stimulation data are shown in Fig. 1. Overall, BOLD and CBF signals increased mostly within the gray matter of the primary visual cortex (indicated by green contours), while CBV-weighted signal decreased due to increasing amounts of iron oxide particles induced by blood vessel dilation. The highest BOLD signal increase (yellow pixels in Fig. 1A) appeared at the cortical surface area with large draining pial veins and cerebrospinal fluid, while the highest CBV-weighted signal changes (purple in Fig. 1B) occurred at the middle cortical area. The CBF response was the highest at the middle cortical area (yellow in Fig. 1C). These findings agree with previous CBV-weighted fMRI studies of the cat visual cortex and rat somatosensory cortex (Harel et al., 2006;

Lu et al., 2004b; Zhao et al., 2006) and CBF data of rat somatosensory cortex (Duong et al., 2000, 2001; Lee et al., 2002).

To examine magnitudes and temporal characteristics of BOLD, CBV and CBF responses, time courses were obtained from the UCA and the MCA (blue and red pixels in Fig. 1D insert image, respectively). Several features were observed. (i) When time courses between two ROIs were compared, the MCA had lower BOLD but higher CBF responses than the UCA, while the peak CBV responses were similar in both areas. (ii) Hemodynamic responses decreased during the stimulation period. The BOLD signal at the MCA dropped relatively faster than that of the UCA, and almost to the pre-stimulus basal level at the end of the stimulation, as also seen in the BOLD map (arrows in Fig. 1A). In contrast, the CBV response was reduced faster at the UCA, where the decay can be separated into two phases: an initial fast decaying phase from the peak to ~20 s after the stimulation onset, and a slow decaying phase from 20 s to the end of the stimulation; the latter phase is similar to the signal decaying characteristics for CBV in the MCA. The CBF time courses in both ROIs were similar. (iii) After the stimulation offset, signal undershoots were consistently observed at both UCA and MCA, for all modalities. The positive peak signal change, intensity and time of the post-stimulus undershoot peak, and ratio of the averaged post-stimulus undershoot between 18 s and 60 s after the stimulation offset to the positive peak intensity are listed in Table 1. The ratio of post-stimulus undershoot to positive peak was significantly less than zero at both MCA and UCA for all three modalities, indicating post-stimulus undershoots exist. For CBV responses, the time to the undershoot peak was much faster in UCA than in MCA ($P<0.05$). For 20-s stimulation data (time courses not shown), a post-stimulus undershoot was seen in the BOLD responses at UCA and MCA, while minute undershoots were observed for CBV at UCA and CBF at MCA.

For each modality, a spatial specificity index can be calculated from its time course that is defined as the ratio of signal changes of MCA to UCA; a higher value indicates that imaging signals are more specific to the middle of the cortex. Three different time periods (TP1: 4–10 s, TP2: 12–30 s, and TP3: 32–60 s) were examined from 60-s stimulation data. Time-dependent specificity indices were summarized for BOLD, CBV, and CBF in Fig. 2. BOLD had the lowest specificity index among the three modalities, and decreased at later time periods from 0.46 in TP1 to 0.31 in TP3. In contrast, the index increased significantly for CBV from 1.0 in TP1 to 3.0 in TP3, and slightly for CBF from 1.4 in TP1 to 1.9 in TP3.

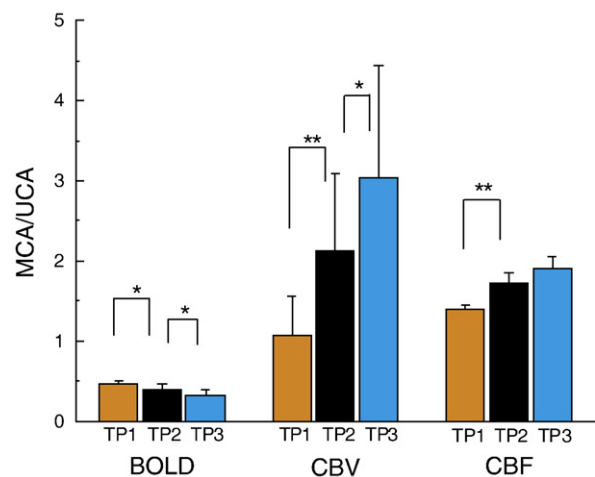


Fig. 2. Time-dependent spatial specificity indices for BOLD, CBV, and CBF. The index was calculated as a ratio of signal changes from the middle to upper cortical area for three time periods during the 60-s stimulation: TP1: 4 to 10 s, TP2: 12 to 32 s and TP3: 32 to 60 s. Statistical differences are indicated as * ($P<0.05$) and ** ($P<0.01$).

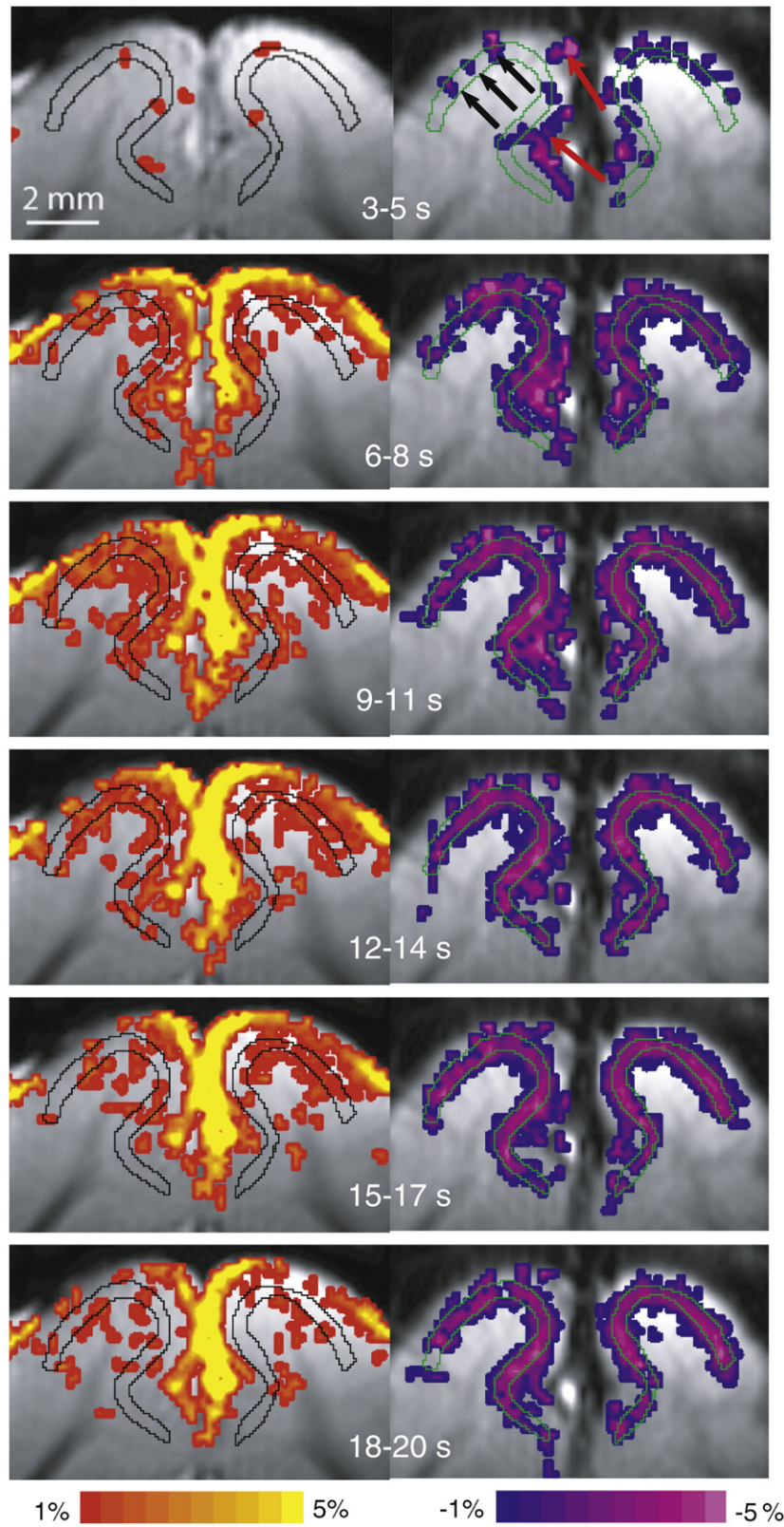


Fig. 3. Time-dependent percentage change maps of BOLD (left) and CBV-weighted (right) fMRI at every 3 s time window for a representative animal. The 20-s stimulation data with TR of 1 s were used with thresholds of $P < 0.05$ and the number of contiguous pixels ≥ 3 . The black and green contours approximately trace the middle of the cortex. Decrease in CBV-weighted signal means an increase in CBV. During stimulation, the CBV change started at the upper cortical layer and then became increasingly localized to the middle cortical layer, whereas the BOLD signal started at the middle of the cortex but became strongest at the cortical surface and cerebrospinal fluid (CSF) area at a later period (> 5 s).

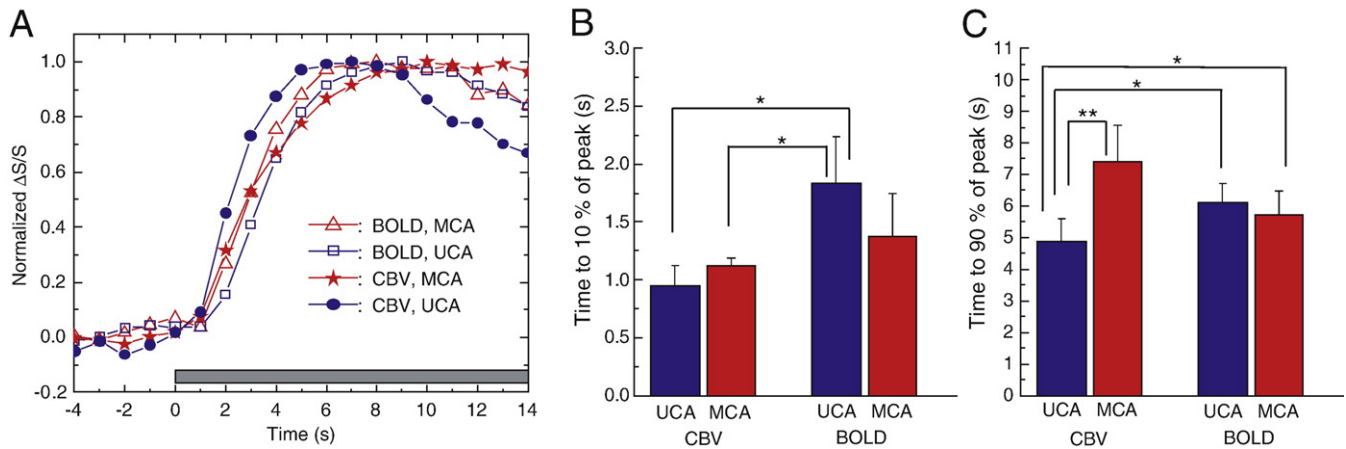


Fig. 4. Dynamic properties of CBV and BOLD responses in the upper and middle cortical areas. (A) Normalized CBV and BOLD time courses with TR of 1 s from the middle and the upper cortical ROI (Fig. 1D, inset image), respectively. The gray bar shows the stimulation period; only data of the initial rising period was shown for better visualization. (B) and (C) Times to 10% and 90% of the peaks. To obtain onset times and times to peak, time courses were linearly interpolated to 200 ms. Statistical differences are indicated as: * ($P < 0.05$), and ** ($P < 0.01$).

Spatiotemporal responses of BOLD and CBV fMRI with TR of 1 s

In order to visualize the time-dependent fMRI responses, functional maps were obtained every 3 s from the 20-s stimulation BOLD

and CBV-weighted data due to their higher temporal resolution (TR=1 s), but not from the 20-s CBF data due to its much lower temporal resolution (Fig. 3). At 3–5 s after the stimulus onset, only a few active pixels were observed in the BOLD map, which were located

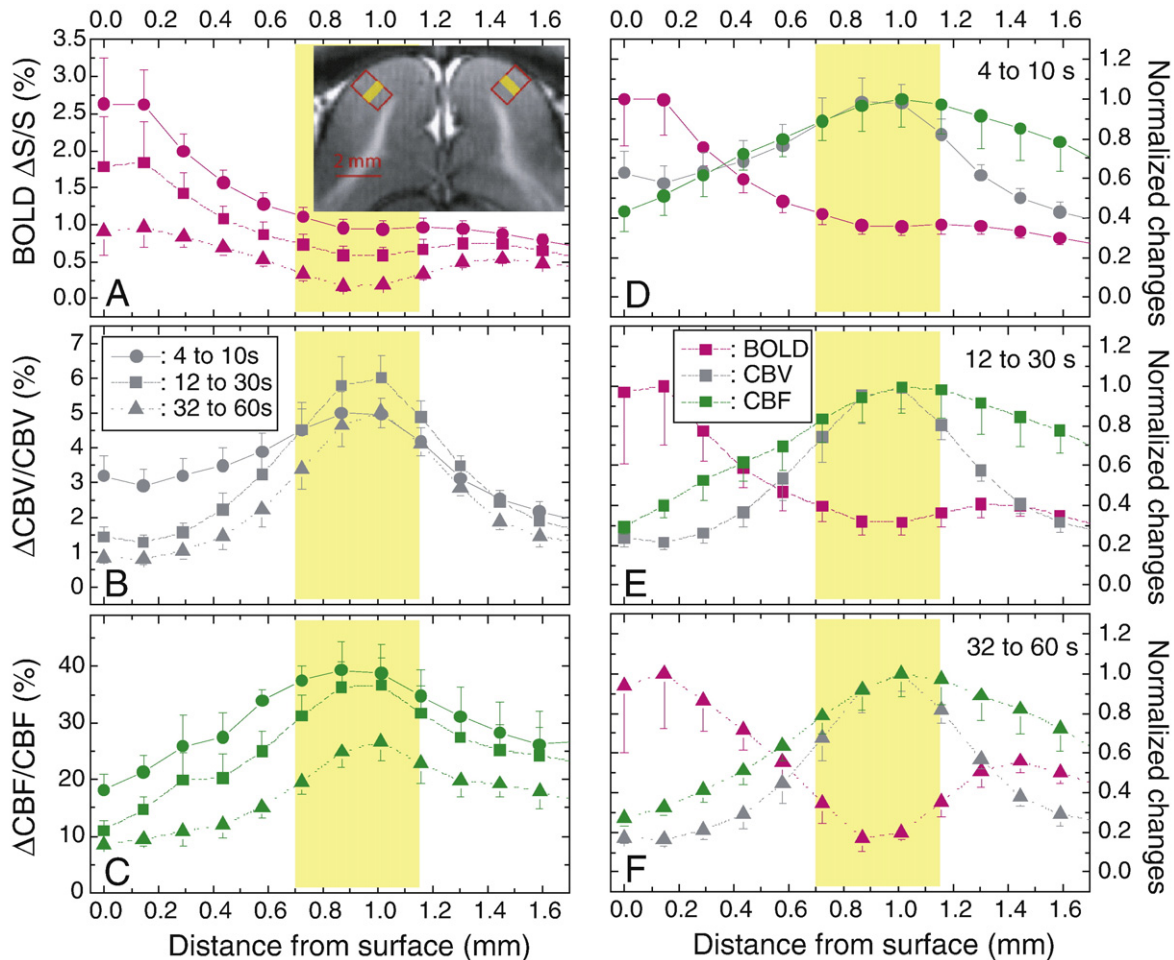


Fig. 5. Cortical-depth profiles of BOLD (A), CBV (B), and CBF (C) responses during three time periods (4 to 10 s, circle; 12 to 30 s, square; and 32 to 60 s, triangle) of the 60-s stimulation data. Profiles were obtained from two rectangle ROIs at area 18 shown in the T_1 -weighted image (inset image). To compare between BOLD, CBV, and CBF, normalized cortical profiles of BOLD (magenta), CBV (gray), and CBF (green) were plotted for the three time periods (D–F). The yellow regions in the background approximately indicate layer 4, which was obtained from literature. Error bar=standard error of the mean.

at or near the middle cortical layer (approximately outlined by black contours); while the CBV-weighted signal change started mostly on the upper cortical area (indicated by the red arrow) and possibly intracortical radial vessels (black arrows). At 6–8 s, large BOLD signals emerged at the cortical surface, while more CBV activated pixels appeared at upper and middle cortical layers. At later times (9–20 s), the strong BOLD signal stayed at the cortical surface, while the CBV response became localized to the middle cortical layer.

To examine detailed dynamic responses of BOLD and CBV signals, time courses were obtained from the upper and middle cortical areas (blue and red pixels in Fig. 1D inset image, respectively). Only the initial rising period in the 20-s stimulation data was plotted in Fig. 4, in addition to the calculated onset times and TTPs. At UCA, the onset of CBV was faster (~ 0.9 s) than that of BOLD. The peak response of CBV at UCA was ~ 1.2 s faster than that of BOLD, and also significantly faster (~ 2.5 s) than CBV at MCA.

Cortical-depth dependence of the BOLD, CBV, and CBF responses

To further quantify the spatiotemporal responses, cortical-depth profiles of BOLD, CBV and CBF responses were calculated from 4–10 s, 12–30 s, and 32–60 s data after the onset of 60-s stimulation (Fig. 5). In agreement with functional maps (see Fig. 1), for all three time periods BOLD responses were the highest in the cortical surface, while CBV and CBF responses were the highest at the middle cortical layer (see yellow highlighted regions which approximately indicate the position of cortical layer 4 (Payne and Peters, 2002)). At the middle of the cortex, the BOLD response decreased significantly during the stimulation. The CBV response in the initial period had a relatively

large change at the upper cortical layer, which decreased significantly for the two later time periods. The cortical-depth profile of CBF response was nearly time-independent, and slightly broader than the CBV profiles (see right column in Fig. 5).

Spatiotemporal relationship between CBF and CBV

The scaling constant γ was calculated from rCBV and rCBF (Fig. 6). A higher γ -value means a larger CBV contribution to CBF change; assuming a plug flow and no blood velocity change during stimulation, the change of CBV is linearly proportional to the change of CBF, e. g. $\gamma=1.0$. In Fig. 6A, γ -value increased after the stimulation onset, reached an initial peak at ~ 5 s in both UCA and MCA, then, changed slightly during the rest of stimulation period. Similar pattern was observed in 20-s stimulation data (not shown). From the cortical-depth profile (Fig. 6B), γ was higher at the upper cortical layer during the initial stimulation period, then the peak shifted to the middle cortical layer. The spatial distribution remained fairly stable for the later time periods, where the γ -value at the middle cortical layer was ~ 2 times larger than that at the upper and deep cortical layers. The mean γ -value across the entire cortex was 0.13–0.15, similar for the three time periods.

Discussions

The major findings in our cortical layer-dependent fMRI studies are: (i) the functional CBV response in the UCA starts and peaks earlier than that of BOLD in the same area. The CBV response in the MCA has longer time to peak compared to the UCA. (ii) The functional responses of BOLD, CBV, and CBF are cortical layer-dependent. Compared to an initial stimulation period (4–10 s), the CBV response at a later time is more localized to the middle cortical layer and is more likely of microvessel origin. (iii) The post-stimulus undershoot is observable in BOLD, CBV and CBF responses for 60-s stimulation, thus post-stimulus BOLD undershoot cannot be explained by a delayed CBV recovery to the baseline. (iv) The relationship between CBV and CBF responses is both cortical layer- and time-dependent.

Temporal dynamics of BOLD, CBV and CBF

Compared to the MCA, the CBV response in the UCA peaked faster during stimulation, and also reached the peak of undershoot faster. Our data support the hypothesis that neural activity directly or indirectly dilates (and constricts after stimulus offset) upstream arterioles first, then downstream vessels including capillaries respond actively or passively in an anterograde manner. Fast-responding arterial vessel dilation is dominant in the UCA, while slow-responding dilation of microvessels contributes to the MCA. Since the delayed CBV response is relatively specific to the middle cortical layer (see Fig. 5B), it may occur at capillaries. This idea is supported by the recent observation of capillary dilation in the rat somatosensory cortex during neural activity (Stefanovic et al., 2008).

The hemodynamic response decreased significantly during the sustained stimulation with our settings. For CBV, decaying from peak response was much faster at the UCA, where a two-phase decaying characteristic supports the existence of fast responding arterial and delayed responding microvessel components (Fig. 3D). In contrast, the decrease of CBF change was only slightly faster in UCA (see Figs. 4 and 5C), likely because the contribution of arterial signals to the CBF response is small. Compared to the UCA, the BOLD signal at MCA dropped faster and nearly reached the baseline, which may be due to a faster decay of CBF with respect to CBV responses at the MCA.

Since the temporal characteristic of CBV differs between the MCA and UCA, the variations of ROI selection can partially be a source of the discrepancies in CBV dynamics reported in the literature. For example, ROIs based on BOLD maps (which contains large vessel

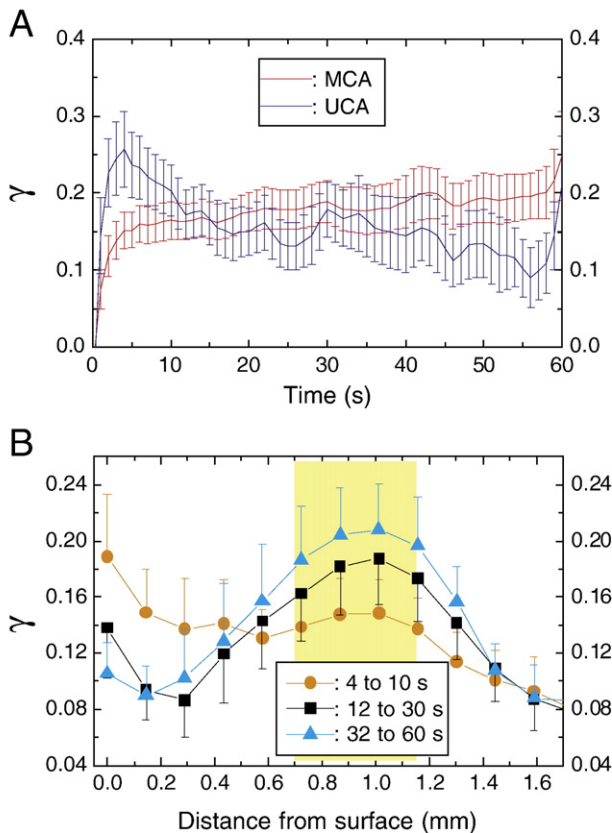


Fig. 6. Relationship between CBF and CBV responses shown as a power-law scaling constant γ . γ was calculated from time courses in Fig. 1 and cortical profiles in Fig. 5. (A) The time course of the power-law scaling constant γ obtained from the middle and upper cortical areas. (B) The cortical-depth profile of γ for three time periods. The highest γ -value was observed in the middle of the cortex. The error bars were calculated by the propagation of error from the CBV and CBF time course data.

regions, see Fig. 1) or based on CBV-weighted fMRI maps (which contains mostly tissue) could change the appearance of dynamic CBV characteristics.

Time dependence of functional maps

Specificity of hemodynamic-based functional maps is time-dependent. The BOLD signal change dominated at surface large vein areas due to their large venous blood volume. Since the BOLD signal propagates from capillaries to large pial veins, the earlier response (3–5 s in Fig. 3) is better localized to neuronal active sites, but has less sensitivity. With a short blood transit time from capillaries to pial veins (<1 s), the cortical layer specificity of our BOLD maps did not change significantly except at the very earliest time (see Fig. 3). These results are consistent with previous findings that the early part of the positive BOLD period originates from the gray matter and can yield well localized functional maps, while at later times (>8–10 s) the BOLD response becomes non-selective (Lee et al., 1995; Menon and Good-year, 1999). On the contrary, since the CBV response propagates from arterial vessels to capillaries and the MCA has a slow and delayed response component which arises presumably from capillaries, the later time points provide much better spatial localization to active sites; thus, the map obtained from the later time period is more specific to the middle cortical layer. Unlike the CBV response that can originate from all sizes of vessels with different time characteristics, the functional CBF signal occurs mostly from capillaries and surrounding tissue, and is, therefore, localized to the MCA with a spatial specificity that is only weakly time-dependent (see Figs. 2 and 5C).

In cat visual stimulation of 2 s duration, non-specific CBV response is dominated in optical imaging; thus, high-resolution maps cannot be easily achieved (Vanzetta et al., 2004). This is consistent with our CBV map obtained 3–5 s after the onset of stimulation (see Fig. 3) which has mostly non-specific signals at upper cortical layer and along the radial vessel direction. In previous CBV studies in the cat visual cortex (Fukuda et al., 2006; Zhao et al., 2005), high specificity maps were obtained from long stimulation data (≥ 10 s). However, our time-dependent CBV results differed from optical imaging studies in the rat somatosensory cortex which found that the initial (<2–3 s) CBV data is optimal for high spatial specificity (Sheth et al., 2004). The discrepancy may be caused by a difference in brain regions (rat barrel cortex vs. cat visual cortex).

Post-stimulus undershoot

The observations of the post-stimulus BOLD undershoot have been found to be dependent on the type of stimulation (Bandettini et al., 1997). Our results indicate that undershoot is also dependent on the stimulation duration. Post-stimulus undershoots were clearly observed in the BOLD, CBV and CBF responses for the 60-s stimulation. For the 20-s stimulation, the undershoot in CBV and CBF is much smaller.

A CBF undershoot was observed for our 60-s stimulation experiments, which is in agreement with a few previous reports (Hoge et al., 1999b; Uludag et al., 2004). Also, the CBV post-stimulus undershoot was detected with similar temporal dynamics and relative magnitude as CBF. Since the CBF signal is regulated by arterial vessels, an undershoot in CBF would imply a post-stimulus decrease in the arterial blood volume, which is likely to be a major contributor for post-stimulus CBV undershoot. Recently, Yacoub et al. studied the post-stimulus responses of BOLD and CBV-weighted signals (with 10 mg/kg MION) using a similar cat visual stimulation model and also found the CBV-weighted signal response (without BOLD correction) is faster at the cortical surface than at tissue area; however, no significant CBV-weighted signal undershoot was observed for their 40-s stimulation study. The apparent discrepancy with our results may be attributable to BOLD contribution to the CBV-weighted signal,

which was reported to be fairly large at 9.4 T from a rat somatosensory study and accounts for 45% and 26% of the CBV-weighted signal change with 5 and 15 mg/kg MION, respectively (Lu et al., 2007). The contribution of post-stimulus negative BOLD signals to CBV-weighted fMRI may appear as sustained CBV increase, which can partially cancel out the actual decrease in CBV.

The BOLD signal can be expressed as: $\Delta S/S \propto CBV_v \cdot \Delta Y - \Delta CBV_v / CBV_v \cdot (1 - Y)$, where CBV_v is the venous blood volume and Y is the oxygenation level. The slow return of venous CBV response to a baseline has been proposed to explain the post-stimulus BOLD undershoot (Buxton et al., 1998; Mandeville et al., 1999b). Under such model, a positive $\Delta CBV_v / CBV_v$ contributes predominantly to the undershoot in BOLD $\Delta S/S$. However, this model disagrees with recent results of human visual stimulation studies using a contrast agent (Frahm et al., 2008) and a vascular space occupancy technique (Lu et al., 2004a). Our data does not support this model either, as a CBV undershoot was observed. Because the venous blood volume consists of >60% of total CBV, it is very unlikely that there is an undershoot in $\Delta CBV / CBV$ with a positive $\Delta CBV_v / CBV_v$.

Spatiotemporal mismatch of the CBV and CBF responses

Our results show that the γ -value is both spatially and temporally dependent during the stimulation, with a higher value at the UCA in the initial period of the stimulation (4–10 s), and later the peak value shifts to the MCA. Since the CBF change is a combination of CBV and velocity changes, the dilation in parenchymal microvessels is more contributed to the middle of the cortex at a later time period compared to upper and lower cortical layers (see Figs. 5E, F). Our γ -value time course in the MCA is, in general, consistent with that observed in the rat somatosensory area, in which the γ -value was 0.13–0.17 for the initial rising period, and 0.19–0.23 for the plateau period during stimulation (Kida et al., 2007). Oxygen metabolism was usually calculated from BOLD and CBF (or CBV) data with a single γ -value, assuming that a significant portion of CBV change is of venous origins (Davis et al., 1998; Kim et al., 1999; Mandeville et al., 1999a; Uludag et al., 2004). For understanding of the dynamic $CMRO_2$ such as in case of short-stimulation or event-related study, the transient behavior of γ -value becomes important. Our results indicate that γ in the rising period is smaller than that obtained from the steady state at the parenchyma. Thus, parenchyma $CMRO_2$ values during the rising period may be overestimated if a steady state γ -value is used.

Our data for the steady state (>10 s) also agree with the rat hypercapnia results of Wu et al. where γ is found to be region-specific (note they used α and $\alpha = 1/\gamma$) (Wu et al., 2002), higher at the parenchyma, and lower at large vessel area. This would imply that the $CMRO_2$ at the parenchyma might be underestimated if γ -values were obtained from very low-resolution study. Interestingly, the mean γ -value across the cortex remained fairly constant during stimulation, suggesting that using a single γ -value at the steady state could be a plausible approximation at very low spatial resolution.

Conclusions

We have studied the cortical layer dependence and the temporal dynamics of BOLD, CBV, and CBF fMRI. The peak CBV response is faster at the upper cortical area than the middle cortical area, suggesting that microvessels take longer time to dilate than larger vessels. The functional maps are dependent on the time window of the stimulation data. For CBV-weighted fMRI, our results indicate that response at a later time period improves the spatial localization of the functional map to the middle cortical area. After the cessation of the stimulus, signal undershoots were consistently observed for BOLD, CBV and CBF for the 60-s stimulation. Thus, the BOLD post-stimulus undershoot cannot be attributed to a slow venous compliance under our conditions. The relationship between CBV and CBF responses shows

spatial and temporal mismatch; therefore, care should be exercised for high-resolution and/or dynamic quantification of oxygen metabolism changes.

Acknowledgments

The authors thank Ping Wang and Michelle Tasker for animal preparation, Kristy Hendrich for 9.4 T supports, Dr. Jicheng Wang for acquiring part of the fMRI data, and Dr. Fuqiang Zhao of Merck & Co., Inc for helpful discussions. This work was supported by NIH grants EB003324, EB003375, and NS44589.

References

- Bandettini, P.A., Kwong, K.K., Davis, T.L., Tootell, R.B.H., Wong, E.C., Fox, P.T., Belliveau, J.W., Weisskoff, R., Rosen, B.R., 1997. Characterization of cerebral blood oxygenation and flow changes during prolonged brain activation. *Hum. Brain Mapp.* 5, 93–109.
- Bonhoeffer, T., Grinvald, A., 1993. The layout of iso-orientation domains in area 18 of cat visual cortex: optical imaging reveals a pin-wheel-like organization. *J. Neurosci.* 13, 4157–4180.
- Buxton, R.B., Wong, E.C., Frank, L.R., 1998. Dynamics of blood flow and oxygenation changes during brain activation: the balloon model. *Magn. Reson. Med.* 39, 855–864.
- Davis, T.L., Kwong, K.K., Weisskoff, R.M., Rosen, B.R., 1998. Calibrated functional MRI: mapping the dynamics of oxidative metabolism. *Proc. Natl. Acad. Sci. U. S. A.* 95, 1834–1839.
- Duong, T.Q., Kim, D.-S., Ugurbil, K., Kim, S.-G., 2001. Localized cerebral blood flow response at submillimeter columnar resolution. *Proc. Natl. Acad. Sci. U. S. A.* 98, 10904–10909.
- Duong, T.Q., Silva, A.C., Lee, S.-P., Kim, S.-G., 2000. Functional MRI of calcium-dependent synaptic activity: cross correlation with CBF and BOLD measurements. *Magn. Reson. Med.* 43, 383–392.
- Frahm, J., Baudewig, J., Kallenberg, K., Kastrup, A., Merboldt, K.D., Dechent, P., 2008. The post-stimulation undershoot in BOLD fMRI of human brain is not caused by elevated cerebral blood volume. *NeuroImage* 40, 473–481.
- Fukuda, M., Moon, C.H., Wang, P., Kim, S.G., 2006. Mapping iso-orientation columns by contrast agent-enhanced functional magnetic resonance imaging: reproducibility, specificity, and evaluation by optical imaging of intrinsic signal. *J. Neurosci.* 26, 11821–11832.
- Garwood, M., Delabarre, L., 2001. The return of the frequency sweep: designing adiabatic pulses for contemporary NMR. *J. Magn. Reson.* 153, 155–177.
- Goodyear, B., Menon, R.S., 2001. Brief visual stimulation allows mapping of ocular dominance in visual cortex using fMRI. *Hum. Brain Mapp.* 14, 210–217.
- Grubb, R.L., Raichle, M.E., Eichling, J.O., Ter-Pogossian, M.M., 1974. The effects of changes in PaCO₂ on cerebral blood volume, blood flow, and vascular mean transit time. *Stroke* 5, 630–639.
- Harel, N., Lee, S.-P., Nagaoka, T., Kim, D.-S., Kim, S.-G., 2002. Origin of negative blood oxygenation level-dependent fMRI signals. *J. Cereb. Blood Flow Metab.* 22, 908–917.
- Harel, N., Lin, J., Moeller, S., Ugurbil, K., Yacoub, E., 2006. Combined imaging-histological study of cortical laminar specificity of fMRI signals. *NeuroImage* 29, 879–887.
- Hoge, R.D., Atkinson, J., Gill, B., Crelier, G.R., Marrett, S., G.B., P., 1999a. Linear coupling between cerebral blood flow and oxygen consumption in activated human cortex. *Proc. Natl. Acad. Sci.* 96, 9403–9408.
- Hoge, R.D., Atkinson, J., Gill, B., Crelier, G.R., Marrett, S., Pike, G.B., 1999b. Stimulus-dependent BOLD and perfusion dynamics in human V1. *NeuroImage* 9, 573–585.
- Jin, T., Wang, P., Tasker, M., Zhao, F.Q., Kim, S.-G., 2006. Source of nonlinearity in echo-time-dependent BOLD fMRI. *Magn. Reson. Med.* 55, 1281–1290.
- Kennan, R.P., Scanley, B.E., Innis, R.B., Gore, J.C., 1998. Physiological basis for BOLD MR signal changes due to neuronal stimulation: separation of blood volume and magnetic susceptibility effects. *Magn. Reson. Med.* 40, 840–846.
- Kida, I., Rothman, D.L., Hyder, F., 2007. Dynamics of changes in blood flow, volume, and oxygenation: implications for dynamic functional magnetic resonance imaging calibration. *J. Cereb. Blood Flow Metab.* 27, 690–696.
- Kim, S.-G., 1995. Quantification of relative cerebral blood flow change by flow-sensitive alternating inversion recovery (FAIR) technique: application to functional mapping. *Magn. Reson. Med.* 34, 293–301.
- Kim, S.-G., Rostrup, E., Larsson, H.B.W., Ogawa, S., Paulson, O.B., 1999. Simultaneous measurements of CBF and CMRO₂ changes by fMRI: Significant increase of oxygen consumption rate during visual stimulation. *Magn. Reson. Med.* 41, 1152–1161.
- Kim, S.-G., Ugurbil, K., 1997. Comparison of blood oxygenation and cerebral blood flow effects in fMRI: Estimation of relative oxygen consumption change. *Magn. Reson. Med.* 38, 59–65.
- Lee, A.T., Glover, G.H., Meyer, C.H., 1995. Discrimination of large venous vessels in time-course spiral blood-oxygen-level-dependent magnetic-resonance functional neuroimaging. *Magn. Reson. Med.* 33, 745–754.
- Lee, S.-P., Silva, A.C., Kim, S.-G., 2002. Comparison of diffusion-weighted high-resolution CBF and spin-echo BOLD fMRI at 9.4 T. *Magn. Reson. Med.* 47, 736–741.
- Leite, F.P., Tsao, D., Vanduffel, W., Fize, D., Sasaki, Y., Wald, L.L., Dale, A.M., Kwong, K.K., Orban, G.A., Rosen, B.R., Tootell, R.B.H., Mandeville, J.B., 2002. Repeated fMRI using iron oxide contrast agent in awake, behaving macaques at 3 Tesla. *NeuroImage* 16, 283–294.
- Lu, H., Golay, X., Pekar, J., van Zijl, P.C., 2004a. Sustained poststimulus elevation in cerebral oxygen utilization after vascular recovery. *J. Cereb. Blood Flow Metab.* 24, 764–770.
- Lu, H.B., Patel, S., Luo, F., Li, S.J., Hillard, C.J., Ward, B.D., Hyde, J.S., 2004b. Spatial correlations of laminar BOLD and CBV responses to rat whisker stimulation with neuronal activity localized by Fos expression. *Magn. Reson. Med.* 52, 1060–1068.
- Lu, H.B., Scholl, C.A., Zuo, Y.T., Stein, E.A., Yang, Y.H., 2007. Quantifying the blood oxygenation level dependent effect in cerebral blood volume-weighted functional MRI at 9.4 T. *Magn. Reson. Med.* 58, 616–621.
- Mandeville, J.B., Marota, J.J., Ayata, C., Moskowitz, M.A., Weisskoff, R.M., Rosen, B.R., 1999a. MRI measurement of the temporal evolution of relative CMRO₂ during rat forepaw stimulation. *Magn. Reson. Med.* 42, 944–951.
- Mandeville, J.B., Marota, J.J.A., Ayata, C., Zaharchuk, G., Moskowitz, M.A., Rosen, B., Weisskoff, R., 1999b. Evidence of a cerebrovascular postarteriole windkessel with delayed compliance. *J. Cereb. Blood Flow Metab.* 19, 679–689.
- Mandeville, J.B., Marota, J.J.A., Kosofsky, B.E., Keltner, J.R., Weissleder, R., Rosen, B.R., 1998. Dynamic functional imaging of relative cerebral blood volume during rat forepaw stimulation. *Magn. Reson. Med.* 39, 615–624.
- Menon, R.S., Goodyear, B.G., 1999. Submillimeter functional localization in human striate cortex using BOLD contrast at 4 Tesla: implications for the vascular point-spread function. *Magn. Reson. Med.* 41, 230–235.
- Ogawa, S., Lee, T.-M., Kay, A.R., Tank, D.W., 1990. Brain magnetic resonance imaging with contrast dependent on blood oxygenation. *Proc. Natl. Acad. Sci. U. S. A.* 87, 9868–9872.
- Payne, B.R., Peters, A., 2002. The concept of cat primary visual cortex. In: Payne, B.R., Peters, A. (Eds.), *The Cat Primary Visual Cortex*. Academic Press, pp. 1–129.
- Sheth, S.A., Nemoto, M., Guiou, M., Walker, M., Pouratian, N., Hageman, N., Toga, A.W., 2004. Columnar specificity of microvascular oxygenation and volume responses: implications for functional brain mapping. *J. Neurosci.* 24, 634–641.
- Silva, A.C., Koretsky, A.P., Duyn, J.H., 2007. Functional MRI impulse response for BOLD and CBV contrast in rat somatosensory cortex. *Magn. Reson. Med.* 57, 1110–1118.
- Stefanovic, B., Hutchinson, E., Yakovleva, V., Schram, V., Russell, J.T., Belluscio, L., Koresky, A.P., Silva, A.C., 2008. Functional reactivity of cerebral capillaries. *J. Cereb. Blood Flow Metab.* 28, 961–972.
- Strupp, J.P., 1996. Stimulate: a GUI based fMRI analysis software package. *NeuroImage* 3, S607.
- Tsao, J., 2003. Interpolation artifacts in multimodality image registration based on maximization of mutual information. *IEEE Trans. Med. Imag.* 22, 854–864.
- Uludag, K., Dubowitz, D.J., Yoder, E.J., Restom, K., Liu, T.T., Buxton, R.B., 2004. Coupling of cerebral blood flow and oxygen consumption during physiological activation and deactivation measured with fMRI. *NeuroImage* 23, 148–155.
- Vanzetta, I., Sloviter, H., Omer, D., Grinvald, A., 2004. Columnar resolution of blood volume and oximetry functional maps in the behaving monkey: implications for fMRI. *Neuron* 42, 843–854.
- Wu, G.H., Luo, F., Li, Z., Zhao, X.L., Li, S.J., 2002. Transient relationships among BOLD, CBV, and CBF changes in rat brain as detected by functional MRI. *Magn. Reson. Med.* 48, 987–993.
- Yacoub, E., Ugurbil, K., Harel, N., 2006. The spatial dependence of the poststimulus undershoot as revealed by high-resolution BOLD- and CBV-weighted fMRI. *J. Cereb. Blood Flow Metab.* 26, 634–644.
- Zhao, F., Wang, P., Hendrich, K., Kim, S.-G., 2005. Spatial specificity of cerebral blood volume-weighted fMRI responses at columnar resolution. *NeuroImage* 27, 416–424.
- Zhao, F., Wang, P., Hendrich, K., Ugurbil, K., Kim, S.-G., 2006. Cortical layer-dependent BOLD and CBV responses measured by spin-echo and gradient-echo fMRI: insights into hemodynamic regulation. *NeuroImage* 30, 1149–1160.